

PAPER • OPEN ACCESS

Effect of piezoelectric patch on natural frequencies of Timoshenko beam made of functionally graded material

To cite this article: Nguyen Tien Khiem *et al* 2020 *Mater. Res. Express* 7 055704

View the [article online](#) for updates and enhancements.



IOP | ebooks™

Bringing together innovative digital publishing with leading authors from the global scientific community.

Start exploring the collection—download the first chapter of every title for free.



PAPER

Effect of piezoelectric patch on natural frequencies of Timoshenko beam made of functionally graded material

OPEN ACCESS

RECEIVED

10 March 2020

REVISED

20 April 2020

ACCEPTED FOR PUBLICATION

28 April 2020

PUBLISHED

11 May 2020

Nguyen Tien Khiem¹ , Tran Thanh Hai² and Luu Quynh Huong³¹ Center for Interdisciplinary Research, Ho Chi Minh City University of Technology (HUTECH), 475A, Dien Bien Phu Str, Binh Thanh Dist., Ho Chi Minh City, Vietnam² Institute of Mechanics, Vietnam Academy of Science and Technology, 264, Doi Can, Ba Dinh, Hanoi, Vietnam³ Faculty of Water Resources Engineering, ThuyLoi University, 175 Tay Son, Dong Da, Hanoi, VietnamE-mail: nt.khiem55@hutech.edu.vn and ntkhiem@imech.vast.vn**Keywords:** functionally graded material, piezoelectric material, modal analysis, Timoshenko beam

Original content from this work may be used under the terms of the [Creative Commons Attribution 4.0 licence](https://creativecommons.org/licenses/by/4.0/).

Any further distribution of this work must maintain attribution to the author(s) and the title of the work, journal citation and DOI.

**Abstract**

The present paper addresses developing the Dynamic Stiffness Method (DSM) for natural frequency analysis of functionally graded beam with piezoelectric patch based on the Timoshenko beam theory and power law of material grading. Governing equations and general solution of free vibration are conducted for the beam element with piezoelectric layer that is modelled as a homogeneous Timoshenko beam. The obtained solution allows establishing dynamic stiffness matrix for modal analysis of FGM beam with bonded piezoelectric distributed sensors/actuators. Effect of thickness and position of the smart sensors/actuators and material parameters on natural frequencies is studied with the aim for dynamic testing and health monitoring of FGM structures. The theoretical developments are validated and illustrated by numerical examples.

1. Introduction

Due to increasingly employed functionally graded materials in high-tech industries, studying behavior of structural components such as beams or plates made of that material under various loadings becomes vitally essential. The most important achievements in modelling and analysis of the material and structures were reported in the surveys given by Birman and Byrd [1] and Gupta and Talha [2]. Various problems in dynamic analysis of functionally graded beams were studied in the widespread literature, for instance, in the works [3–7]. A large number of works is devoted also to study vibrations of the beams with localized damages such as cracks [8–13]. Recently, some procedures were proposed by Yu and Chu [14]; Banerjee *et al* [15] and Khiem and Huyen [16] to detect cracks in functionally graded beams with natural frequencies measured by the traditional technique of modal testing. As well known, the traditional modal testing is restricted to use a limited number of discrete sensors and actuators that are usually unable to gather sufficient amount of data for solving the problem of damage detection in structural health monitoring. Therefore, using distributed sensors and actuators for modal testing would be surely promising to enhance solution of the damage detection problem.

Tzou and Tseng [17] demonstrated the necessity in using distributed piezoelectric sensor/actuator for dynamic measurement/control of distributed parameter systems such as flexible structures. The authors have developed also the so-called piezoelectric finite element approach to free vibration of a plate with distributed piezoelectric actuator on the top and sensor at the bottom. Lee and moon [18] developed a theory of distributed sensor/actuator that can be adopted to measure/excite specific modes of plates and beams. Rao and Sunar [19] accomplished a comprehensive survey on the use of piezoelectric materials for disturbance sensing and control of flexible structures. Lee and Jiang [20] studied the electromechanical properties of a piezoelectric laminae that can be used as distributed sensor/actuator for measurement/control of the distributed parameter systems. Recent progress in structural health monitoring by the use of distributed piezoelectric transducers was reported in [21, 22]. Particularly, Wang and Quek [23] showed that the buckling and flutter capacities of an elastic column could be enhanced by using piezoelectric patches bonded to both sides of the column as actuators with an

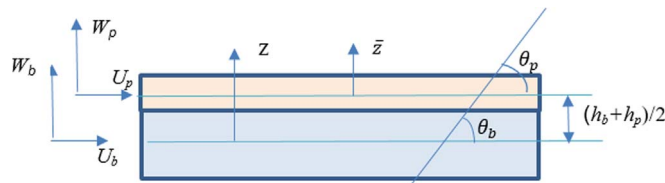


Figure 1. FGM beam element with piezoelectric layer.

applied voltage. Wang *et al* [24] revealed an effect of a piezoelectric patch bonded to a beam on natural frequency of the beam and demonstrated an interesting fact that piezoelectric patch used as an actuator could restore the healthy condition of a cracked beam. Mateescu *et al* [25] presented a method for crack detection in beam and plate using piezoelectric sensors bonded on both sides of the structures.

Using piezoelectric material for sensing and controlling a structure behavior is essentially leading to analysis of the structures with piezoelectric components [26, 27] such as beams or plates with layers or patches. Namely, Yang and Lee [28] used the stepped beam model for modal analysis of Timoshenko beam with piezoelectric patches symmetrically bonded onto both the top and bottom and demonstrated that stiffness and inertia of the piezoelectric material, as well as shear deformation and rotary inertia of the base beam may make change in natural frequencies of the coupled beam. The model of multistep beam was employed also by Maurini *et al* [29] for modal analysis of classical beam with numerous pairs of piezoelectric patches using different techniques including the so-called assumed modes method proposed by themselves. Wang and Quek [30] used the sandwich beam model for modal analysis of a Euler–Bernoulli beam embedded with piezoelectric layers and they found that natural frequency of the sandwich beam is function of stiffness and thickness of the piezoelectric layers. Lee and Kim [31] first proposed to apply the spectral element method (SEM) for vibration analysis of also Euler–Bernoulli beam bonded with a piezoelectric layer (two-layer beam model) and declared that the SEM may provide reliable dynamic characteristics of the elastic-piezoelectric two-layer beams. Then, the SEM have been developed for modelling and analysis of homogeneous [32] and composite [33] Timoshenko beams with piezoelectric layers.

While the most of the aforementioned studies are concerned with the homogeneous beams, there is found in the literature very few works devoted to functionally graded beams with piezoelectric patches except some mentioned below. The stability of an FGM Timoshenko beam embedded by the top and bottom piezoelectric layers/actuators has been investigated in [34] and it is found a significant effect of both the piezoelectric actuators and FGM parameters on the critical buckling loads. Li *et al* [35] even proposed a model of functionally graded piezoelectric beam for its vibration analysis and revealed the increase of natural frequency and decrease of electric potential with increasing gradient index of the material. Recently, Bendine *et al* [36] studied the problem for active vibration control of functionally graded beams with upper and lower surface-bonded piezoelectric layers using the finite element method.

The present paper addresses developing the Dynamic Stiffness Method (DSM) for natural frequency analysis of functionally graded Timoshenko beam with a bonded piezoelectric patch. The DSM is preferred to develop herein because of the following reasons. First, DSM allows one to obtain response of a structure in arbitrarily high-frequency range that is typical for piezoelectric material. Second, when a number of piezoelectric patches are bonded to a uniform beam it becomes nonuniform one of stepwise varying cross section, for analysis of which the DSM is most efficient. Thus, the subject of this study is to examine the effect of thickness and location of the piezoelectric patch mutually with gradient index of the material on the beam's natural frequencies in different cases of boundary conditions. Theoretical development is validated and illustrated by numerical results.

2. Governing equations

Consider an FGM beam of length L , cross sectional area $A_b = b \times h_b$ (figure 1). It is assumed that the material properties of the beam vary along the thickness direction by the power law distribution as follows

$$\mathfrak{R}(z) = \mathfrak{R}_b + (\mathfrak{R}_t - \mathfrak{R}_b)(z/h + 0.5)^n; \quad -h_b/2 \leq z \leq h_b/2, \quad (1)$$

where \mathfrak{R} stands for Young's, shear modulus and material density E , G , ρ ; subscripts t and b denote the top and bottom material respectively; n is power law exponent; z is ordinate of point along the beam height from the mid plane. Assuming small deformation in the framework of Timoshenko beam theory, the constituting equations

for the beam at section x are

$$\begin{aligned} u(x, z, t) &= u_0(x, t) - (z - h_0)\theta(x, t); \\ w(x, z, t) &= w_0(x, t); \\ \sigma_x &= E(z)\varepsilon_x; \tau_{xz} = G(z)\gamma_{xz} \\ \varepsilon_x &= \partial u_0 / \partial x - (z - h_0)\partial \theta / \partial x; \gamma_{xz} = \partial w_0 / \partial x - \theta, \end{aligned} \quad (2)$$

where $u(x, z, t)$, $w(x, z, t)$ are axial and transverse displacements in cross-section at x ; $u_0(x, t)$, $w_0(x, t)$ are the displacements on the neutral plane and θ is rotation of the cross-section; ε_x , γ_{xz} , σ_x , τ are deformation and strain components; κ is geometry correction factor; h_0 is acknowledged as exact position of neutral plane measured from the beam midplane. Based on the condition for neutral plane of the FGM beam, the actual position of neutral axis is calculated as

$$h_0 = n(r_e - 1)h/2(n + 2)(n + r_e); r_e = E_t/E_b. \quad (3)$$

Using the constitutive equation (2) strain energy of the beam is calculated as

$$\begin{aligned} \Pi_b &= (1/2) \int \int \int (\sigma_x \varepsilon_x + \tau_{xz} \gamma_{xz}) dV_b \\ &= (1/2) \int \int \int [E(z)\varepsilon_x^2 + \kappa G(z)\gamma_{xz}^2] dV_b \\ &= \int_L^0 \left\{ A_{11}u_0'^2 - 2A_{12}u_0'\theta' + A_{22}\theta'^2 + \right. \\ &\quad \left. + A_{33}(w_0' - \theta)^2 \right\} dx, \end{aligned} \quad (4)$$

where comma denotes derivative with respect to spatial variable x and

$$\begin{aligned} A_{11} &= \int_A E(z) dA = bhE_b \varphi_1(r_e, n); \\ A_{12} &= \int_A E(z)(z - h_0) dA = bh^2E_b \varphi_2(r_e, n); \\ A_{22} &= \int_A E(z)(z - h_0)^2 dA = bh^3E_b \varphi_3(r_e, n); \\ A_{33} &= \kappa \int_A G(z) dA = bh\kappa G_b \varphi_1(r_g, n); \\ \varphi_1(x, n) &= (x + n)/(1 + n); \varphi_2(x, n) \\ &= (2x + n)/2(2 + n) - \alpha(x + n)/(1 + n) \\ r_\rho &= \rho_t/\rho_b; r_e = E_t/E_b; r_g = G_t/G_b; \alpha = 1/2 + h_0/h_b \end{aligned} \quad (5)$$

On the other hand, kinetic energy of the beam is

$$\begin{aligned} T_b &= (1/2) \int \int \int \rho(\dot{u}^2 + \dot{w}^2) dV \\ &= (1/2) \int_0^L \{ I_{11}\dot{u}_0^2 - 2I_{12}\dot{u}_0\dot{\theta} + I_{22}\dot{\theta}^2 + I_{11}\dot{w}_0^2 \} dx \end{aligned} \quad (6)$$

with

$$\begin{aligned} I_{11} &= \int_A \rho(z) dA = bh_b \rho_b \varphi_1(r_\rho, n); \\ I_{12} &= \int_A \rho(z)(z - h_0) dA = bh_b^3 \rho_b \varphi_2(r_\rho, n); \\ I_{22} &= \int_A \rho(z)(z - h_0)^2 dA = bh_b^3 \rho_b \varphi_3(r_\rho, n). \end{aligned} \quad (7)$$

Let's now consider the piezoelectric layer as a homogeneous Timoshenko beam element, so that constitutive equations can be expressed as

$$\begin{aligned} u_p(x, \bar{z}, t) &= u_{p0}(x, t) - \bar{z}\theta_p(x, t), w_p(x, \bar{z}, t) = w_{p0}(x, t) \\ \varepsilon_{px} &= u_{p0}' - \bar{z}\theta_p', \gamma_p = w_{p0}' - \theta_p \\ \sigma_{px} &= C_{11}^p \varepsilon_{px} - h_{13}D; \tau_p = C_{55}^p \gamma_p; \varepsilon = -h_{13}\varepsilon_{px} + \beta_{33}^p D, \end{aligned} \quad (8)$$

where C_{11}^p , h_{13} , β_{33}^p are elastic modulus, piezoelectric and dielectric constants respectively. ε and D are electric field and displacement of the piezoelectric layer.

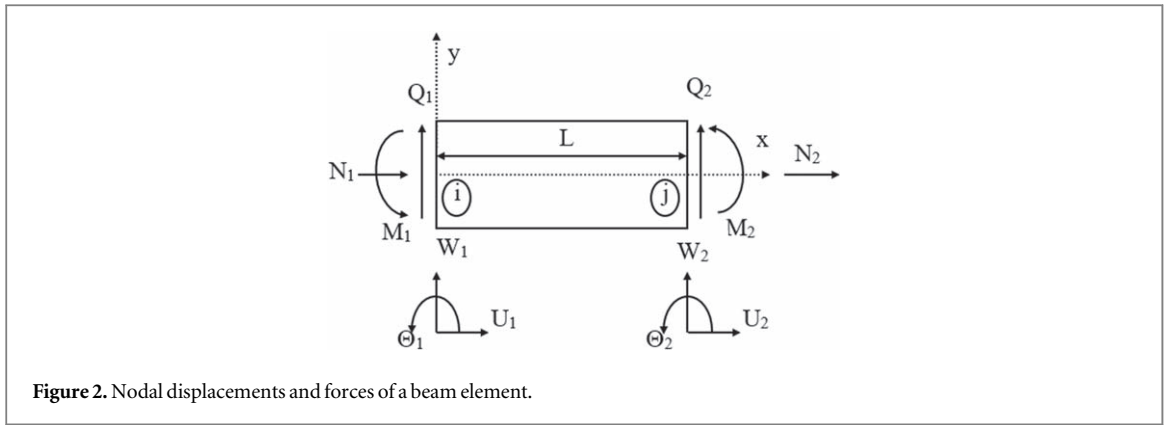


Figure 2. Nodal displacements and forces of a beam element.

Perfect bonding of the base beam with the piezoelectric layer is represented by the conditions

$$u\left(x, \frac{h_b}{2}, t\right) = u_p\left(x, -\frac{h_p}{2}, t\right), w\left(x, \frac{h_b}{2}\right) = w_p(x, -h_p/2, t), \tag{9}$$

that yield

$$u_{p0} = u_0 - \theta h/2, h = h_b + h_p, w_{p0} = w_0, \theta = \theta_p. \tag{10}$$

Therefore

$$\varepsilon_{px} = u'_0 - (\bar{z} + h/2)\theta', \gamma_p = w'_0 - \theta; \tag{11}$$

and

$$\begin{aligned} \Pi_p &= (1/2) \int \int \int (\sigma_{px}\varepsilon_{px} + \tau_p\gamma_p + \varepsilon D) dV_p \\ &= (1/2) \int \int \int [C_{11}^p \varepsilon_{px}^2 - 2h_{13}D\varepsilon_{px} + C_{55}^p \gamma_p^2 + \beta_{33}^p D^2] dV_p \\ &= (1/2) \int_0^L \left\{ \begin{aligned} &C_{11}^p A_p u_0'^2 - C_{11}^p A_p h u_0' \theta' + \\ &C_{11}^p (I_p + A_p h^2/4) \theta'^2 + C_{55}^p A_p (w_0' - \theta)^2 \end{aligned} \right\} dx \\ &\quad - (1/2) \int_0^L \{2h_{13}A_p D(u_0' - h\theta'/2) - \beta_{33}^p A_p D^2\} dx; \\ T_p &= (1/2) \int \int \int \rho_p (\dot{u}_p^2 + \dot{w}_p^2) dV \\ &= (1/2) \int_0^L \left\{ \begin{aligned} &\rho_p A_p \dot{u}_0^2 - \rho_p A_p h \dot{u}_0 \dot{\theta} \\ &+(\rho_p I_p + \rho_p A_p h^2/4) \dot{\theta}^2 + \rho_p A_p \dot{w}_0^2 \end{aligned} \right\} dx, \end{aligned} \tag{12}$$

where $A_p = bh_p$; $I_p = bh_p^3/12$. Therefore, total strain and kinetic energies of the system are

$$\begin{aligned} \Pi &= \Pi_b + \Pi_p \\ &= (1/2) \int_0^L \left\{ \begin{aligned} &A_{11}^* u_0'^2 - 2A_{12}^* u_0' \theta' + A_{22}^* \theta'^2 + \\ &A_{33}^* (w_0' - \theta)^2 \\ &-2h_{13}A_p D(u_0' - h\theta'/2) + \beta_{33}^p A_p D^2 \end{aligned} \right\} dx, \\ T &= T_b + T_p = (1/2) \int_0^L \left\{ \begin{aligned} &I_{11}^* \dot{u}_0^2 - 2I_{12}^* \dot{u}_0 \dot{\theta} \\ &+ I_{22}^* \dot{\theta}^2 + I_{11}^* \dot{w}_0^2 \end{aligned} \right\} dx, \end{aligned} \tag{13}$$

where

$$\begin{aligned} A_{11}^* &= A_{11} + C_{11}^p A_p; A_{12}^* = A_{12} + C_{11}^p A_p h/2; \\ A_{22}^* &= A_{22} + C_{11}^p (I_p + A_p h^2/4); A_{33}^* = \kappa A_{33} + C_{55}^p A_p; \\ I_{11}^* &= I_{11} + \rho_p A_p; I_{12}^* = I_{12} + \rho_p A_p h/2; \end{aligned} \tag{14a}$$

$$I_{22}^* = I_{22} + \rho_p I_p + \rho_p A_p h^2/4. \tag{14b}$$

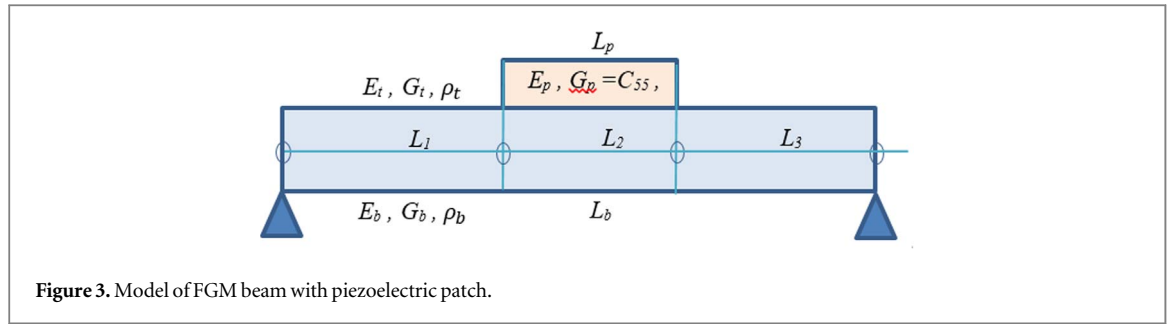


Figure 3. Model of FGM beam with piezoelectric patch.

Putting expressions (13) to the Hamilton's principle

$$\int_{t_1}^{t_2} \delta(T - \Pi) dt = 0,$$

one gets

$$\begin{aligned} (I_{11}^* \ddot{u}_0 - A_{11}^* u_0') - (I_{12}^* \ddot{\theta} - A_{12}^* \theta') + h_{13} A_p D' &= 0; \\ I_{11}^* \ddot{w}_0 - A_{33}^* (w_0' - \theta') &= 0 \\ (I_{12}^* \ddot{u}_0 - A_{12}^* u_0') - (I_{22}^* \ddot{\theta} - A_{22}^* \theta') + (A_{33}^* (w_0' - \theta) + h_{13} A_p h D')/2 &= 0; \\ h_{13} A_p (u_0' - h\theta'/2) - \beta_{33}^p A_p D &= 0 \end{aligned} \tag{15a}$$

and

$$\begin{aligned} [(A_{11}^* u_0' - A_{12}^* \theta' + h_{13} A_p D) \delta u_0]_0^L &= 0; \\ [(A_{21}^* u_0' - A_{22}^* \theta' + h_{13} A_p h D/2) \delta \theta]_0^L &= 0; \\ [(A_{33}^* (w_0' - \theta) \delta w_0]_0^L &= 0. \end{aligned} \tag{15b}$$

The last equation in (15a) allows one to find $D = h_{13}(u_0' - h\theta'/2)/\beta_{33}^p$, so that remaining equations in (15) can be written as

$$\begin{aligned} (I_{11}^* \ddot{u}_0 - B_{11}^* u_0'') - (I_{12}^* \ddot{\theta} - B_{12}^* \theta'') &= 0; \\ (I_{12}^* \ddot{u}_0 - B_{12}^* u_0'') - (I_{22}^* \ddot{\theta} - B_{22}^* \theta'') + A_{33}^* (w_0' - \theta) &= 0; \\ I_{11}^* \ddot{w}_0 - A_{33}^* (w_0'' - \theta') &= 0, \end{aligned} \tag{16}$$

and

$$\begin{aligned} [(B_{11}^* u_0' - B_{12}^* \theta') \delta u_0]_0^L &= 0; \\ [(B_{21}^* u_0' - B_{22}^* \theta') \delta \theta]_0^L &= 0; \\ [(A_{33}^* (w_0' - \theta) \delta w_0]_0^L &= 0, \end{aligned}$$

where the constants $B_{11}^*, B_{12}^*, B_{22}^*$ are

$$\begin{aligned} B_{11}^* &= A_{11}^* - A_p h_{13}^2 / \beta_{33}^p = A_{11} + E_p A_p, \\ B_{12}^* &= A_{12}^* - A_p h h_{13}^2 / 2\beta_{33}^p = A_{12} + E_p A_p h / 2, \\ B_{22}^* &= A_{22}^* - A_p h^2 h_{13}^2 / 4\beta_{33}^p = A_{22} + C_{11}^p I_p + E_p A_p h^2 / 4; \\ E_p &= C_{11}^p - h_{13}^2 / \beta_{33}^p. \end{aligned}$$

Transferring equation (16) into the frequency domain, one gets

$$[\mathbf{A}]\{\mathbf{Z}''(x, \omega)\} + [\mathbf{B}]\{\mathbf{Z}'(x, \omega)\} + [\mathbf{C}]\{\mathbf{Z}(x, \omega)\} = 0, \tag{17}$$

where vectors

$$\begin{aligned} \mathbf{Z} &= \{U(x, \omega), \Theta(x, \omega), W(x, \omega)\}^T \\ &= \int_{-\infty}^{\infty} \{u_0(x, t), \theta(x, t), w_0(x, t)\} e^{-i\omega t} dt, \\ \mathbf{Z}' &= d\mathbf{Z}/dx, \mathbf{Z}'' = d^2\mathbf{z}/dx^2, \end{aligned}$$

Table 1. Frequency parameter $\lambda = \omega(L^2/h)\sqrt{\rho_b/E_b}$ of SS-beam for various thickness of intermediate piezoelectric patch in different gradient index (n) and $L_b/h_b = 10$.

N	Reference [6]	Thickness ratio (h_p/h_b)							Mode No.
		0	0.1	0.2	0.3	0.5	0.8	1.0	
0.1	5.0001	4.9977	4.8389	4.7306	4.6613	4.6000	4.5877	4.5793	1
	19.136	19.1228	18.9199	18.7562	18.6240	18.4157	18.1159	17.8641	2
	40.385	40.3570	39.7208	39.3880	39.2974	39.6770	63.4179	39.1969	3
	56.379	56.3731	53.5208	51.0267	48.8414	45.2184	88.3986	42.5163	4
	66.608	66.5611	65.1948	64.2781	63.7096	63.2773	104.2558	63.5687	5
0.2	4.7348	4.7243	4.5925	4.5055	4.4532	4.4160	4.4234	4.4222	1
	18.118	18.0772	17.9094	17.7774	17.6735	17.5129	17.2723	17.0590	2
	38.240	38.1525	37.623	37.3645	37.3264	37.7672	39.2921	37.8191	3
	53.361	53.5455	051.0074	48.7679	46.7881	43.4665	39.7020	40.5997	4
	63.075	62.9317	61.7907	61.0465	60.6120	60.3645	60.6528	60.8573	5
0.5	4.2432	4.2086	4.1227	4.0725	4.0496	4.0539	4.0947	4.1054	1
	16.235	16.1021	15.9932	15.9140	15.8568	15.7739	15.6287	15.4782	2
	34.261	33.9801	33.6327	33.5033	33.5575	34.1035	35.6428	34.9610	3
	48.044	48.0050	46.0115	44.2240	42.6177	39.8608	36.6288	36.8898	4
	56.502	56.0479	55.2834	54.8306	54.6220	54.6816	55.2047	55.4950	5
1.0	3.8586	3.8004	3.7466	3.7223	3.7201	3.7532	3.8162	3.8347	1
	14.755	14.5331	14.4646	14.4212	14.3951	14.3625	14.2788	14.1702	2
	31.110	30.6491	30.4283	30.3897	30.5077	31.1190	32.6381	32.2887	3
	43.242	43.1884	41.5954	40.1492	38.8330	36.5316	33.7576	33.8135	4
	51.256	50.5213	50.0108	49.7536	71.7626	49.9431	50.5904	50.9232	5
2.0	3.551	3.4878	3.4560	3.4494	3.4612	3.5132	3.5905	3.6144	1
	13.561	13.3229	13.2820	13.2624	13.2565	13.2560	13.2122	13.1318	2
	28.544	28.0555	27.9209	27.9422	28.0992	28.7384	30.2021	29.7505	3
	38.958	38.9090	37.6169	36.4329	35.3445	33.4138	31.0353	31.2956	4
	46.941	46.1729	45.8284	45.6945	65.8800	46.0678	46.7499	47.0885	5
5.0	3.2608	3.2251	3.2099	3.2164	3.2382	3.3034	3.3898	3.4173	1
	12.434	12.3013	12.2811	12.2789	12.2872	12.3085	12.2915	12.2309	2
	26.122	25.8533	25.7836	25.8495	26.0339	26.6842	28.0790	27.2950	3
	35.052	35.0281	33.9649	32.9840	32.0756	30.4476	28.4107	29.0882	4
	42.873	42.4555	42.2318	42.1847	60.7640	42.6634	43.3332	43.6556	5
10	3.0959	3.0805	3.0736	3.0869	3.1140	3.1856	3.2750	3.3028	1
	11.805	11.7476	11.7377	11.7440	11.7590	11.7897	11.7823	11.7288	2
	24.799	24.6834	24.6488	24.7419	24.9464	25.6174	26.9992	26.1886	3
	33.371	33.3619	32.3844	31.4805	30.6412	29.1317	27.2334	27.9769	4
	40.700	40.5218	40.3637	40.3679	58.1686	40.9218	41.5962	41.9124	5

and matrices

$$[\mathbf{A}] = \begin{bmatrix} B_{11}^* & -B_{12}^* & 0 \\ -B_{12}^* & B_{22}^* & 0 \\ 0 & 0 & A_{33}^* \end{bmatrix};$$

$$[\mathbf{B}] = \begin{bmatrix} 0 & 0 & 0 \\ 0 & 0 & A_{33}^* \\ 0 & -A_{33}^* & 0 \end{bmatrix};$$

$$[\mathbf{C}] = \begin{bmatrix} \omega^2 I_{11}^* & -\omega^2 I_{12}^* & 0 \\ -\omega^2 I_{12}^* & \omega^2 I_{22}^* - A_{33}^* & 0 \\ 0 & 0 & \omega^2 I_{11}^* \end{bmatrix}$$

If the piezoelectric layer is employed as a distributed sensor, charge output of which can be calculated as

$$Q = \int D dA = b \int_0^L D dx = (bh_{13}/\beta_{33}^p)(u_0 - h\theta/2)_0^L \quad (18)$$

Table 2. Frequency parameter $\lambda = \omega(L^2/h)\sqrt{\rho_b/E_b}$ of CC-beam for various thickness of intermediate piezoelectric patch in different gradient index (n) and $L_b/h_b = 10$.

N	Reference [6]	Thickness ratio (h_p/h_b)							Mode No.
		0	0.1	0.2	0.3	0.5	0.8	1.0	
0.1	10.82	10.8205	10.3073	9.9140	9.6138	9.2118	8.8843	8.7383	1
	727.809	27.7924	27.3374	26.9592	26.6431	26.1204	25.3414	24.6945	2
	50.364	50.3343	49.7159	49.3971	48.9573	45.4864	41.8199	40.1899	3
	56.379	56.3731	53.5391	51.0869	49.3198	49.7346	51.3394	52.7708	4
	76.611	76.5667	75.1039	74.1304	73.5402	73.1408	73.4384	73.7288	5
0.2	10.253	10.2319	9.7867	9.4459	9.1873	8.8451	8.5707	8.4457	1
	26.337	26.2854	25.9019	25.5884	25.3306	24.9093	24.2638	23.7051	2
	47.704	47.6118	47.1022	46.8619	46.8433	43.692	40.2557	38.6977	3
	53.561	53.5455	51.0221	48.8170	46.8839	947.3356	48.9906	50.4250	4
	72.577	72.4358	71.2142	70.4244	69.9750	69.7644	70.1943	70.5147	5
0.5	9.1864	9.1182	8.7889	8.5397	8.3543	8.1188	7.9387	7.8508	1
	23.594	23.4254	23.1619	22.9567	22.7957	22.5405	22.1139	21.7043	2
	42.727	42.4315	42.106	42.0014	42.0834	40.0176	37.0387	35.6358	3
	48.044	48.0050	646.0206	44.2553	42.6807	42.7030	44.4172	45.8270	4
	64.989	64.5588	63.7416	63.2643	63.0557	63.1656	63.8138	64.1851	5
1.0	8.3437	8.2292	7.9819	7.7984	7.6661	7.5079	7.3957	7.3344	1
	21.404	21.1256	20.9450	20.8134	20.7171	20.5705	20.2868	19.9786	2
	38.721	38.2389	38.0419	38.0302	38.1797	36.6395	34.0633	32.8117	3
	43.242	43.1884	41.6006	40.1683	38.8731	38.8741	40.5855	41.9358	4
	58.840	58.1469	57.6043	57.3389	57.2907	57.6024	58.3681	58.7625	5
2.0	7.6610	7.5376	7.3478	7.2107	7.1157	7.0112	6.9452	6.9023	1
	19.608	19.3119	19.1879	19.1053	19.0510	18.9730	18.7803	18.5397	2
	35.398	34.8940	34.7836	34.8325	35.0216	33.4871	31.2654	30.1613	3
	38.958	38.9091	37.6193	36.4435	35.3688	35.7445	37.3983	38.6618	4
	53.695	52.9791	52.6171	52.4857	52.5324	52.9447	53.7380	54.1268	5
5.0	7.0184	6.9493	6.8031	6.7011	6.6342	6.5694	6.5364	6.5066	1
	17.909	17.7560	17.6738	17.6263	17.6010	17.5682	17.4348	17.2402	1
	32.279	32.0050	31.9598	32.0532	32.0909	30.4996	28.5903	27.6276	3
	35.052	35.0282	33.9660	32.9900	32.2690	32.9997	34.5735	35.7399	4
	48.873	48.4886	48.2580	48.2204	48.3283	48.7891	49.5618	49.9273	5
10	6.6638	6.6339	6.5082	6.4234	6.3705	6.3259	6.3086	6.2843	1
	17.014	16.9432	16.8812	16.8507	16.8392	16.8264	16.7160	16.5396	2
	30.647	30.5295	30.5198	30.6407	30.6548	29.1786	27.3983	26.4960	3
	33.371	33.3620	32.3855	31.4858	30.8771	31.6291	33.1894	34.3221	4
	46.401	46.2376	46.0778	46.0955	46.2437	46.7463	47.5239	47.8816	5

3. Dynamic stiffness matrix for FGM beam element with piezoelectric layer

3.1. General solution of vibration in FGM beam with piezoelectric layer

Seeking solutions of equation (17) in the form: $Z_0 = de^{\lambda x}$ leads to characteristic equation

$$\det[\lambda^2 A + \lambda B + C] = 0 \tag{19}$$

This is in fact a cubic algebraic equation with respect to $\eta = \lambda^2$ that can be easily solved to give three roots η_1, η_2, η_3 , so that one obtains

$$\lambda_{1,4} = \pm k_1; \lambda_{2,5} = \pm k_2; \lambda_{3,6} = \pm k_3; k_j = \sqrt{\eta_j}, j = 1, 2, 3.$$

As a consequence, general solution of equation (17) is represented as

$$\begin{aligned} \{z_0\} &= \begin{bmatrix} d_{11} & d_{12} & \dots & d_{16} \\ d_{21} & d_{22} & \dots & d_{26} \\ d_{31} & d_{32} & \dots & d_{36} \end{bmatrix} \cdot \begin{Bmatrix} e^{\lambda_1 x} \\ \vdots \\ e^{\lambda_6 x} \end{Bmatrix} \\ &= \begin{bmatrix} \alpha_1 C_1 & \alpha_2 C_2 & \dots & \alpha_6 C_6 \\ C_1 & C_2 & \dots & C_6 \\ \beta_1 C_1 & \beta_2 C_2 & \dots & \beta_6 C_6 \end{bmatrix} \cdot \begin{Bmatrix} e^{\lambda_1 x} \\ \vdots \\ e^{\lambda_6 x} \end{Bmatrix} \end{aligned}$$

Table 3. Frequency parameter $\lambda = \omega(L^2/h)\sqrt{\rho_b/E_b}$ of CF-beam for various thickness of intermediate piezoelectric patch in different gradient index (n) and $L_b/h_b = 10$.

Index n	Reference [6]	Thickness ratio (h_p/h_b)							Mode No.
		0	0.1	0.2	0.3	0.5	0.8	1.0	
0.1	1.7966	1.7954	1.7771	1.7608	1.7458	1.7169	1.6711	1.6383	1
	10.782	10.7744	10.4733	10.2903	10.2012	10.2243	10.5215	10.7624	2
	28.190	28.1583	27.2746	26.4421	25.6609	24.2303	22.3441	21.2295	3
	28.404	28.4174	28.1901	28.0659	28.0285	28.1543	28.6475	29.0841	4
	51.618	51.5826	50.8910	50.5109	50.3793	50.6939	52.1539	53.4942	5
0.2	1.7010	1.6972	1.6819	1.6685	1.6561	1.6319	1.5922	1.5630	1
	10.208	10.1850	9.9345	9.7887	9.7271	9.7834	10.0946	10.3315	2
	26.781	26.6685	25.9008	25.1714	24.4810	23.1999	21.4769	20.4420	3
	26.895	26.9501	26.7631	26.6716	26.6595	26.8152	27.3132	27.7369	4
	48.878	48.7694	48.1946	47.8987	47.8301	48.2289	49.7489	51.0999	5
0.5	1.5244	1.5120	1.5019	1.4932	1.4852	1.4689	1.4395	1.4166	1
	9.1477	9.0719	8.9075	8.8265	8.8128	8.9265	9.2584	9.4851	2
	24.024	23.7474	23.2129	22.6726	22.1453	21.1336	19.7125	18.8307	3
	24.098	24.1860	24.0317	23.9834	24.0077	24.2043	24.6946	25.0840	4
	43.787	43.4392	43.0616	42.9099	42.9490	43.4870	45.0843	46.4249	5
1.0	1.3864	1.3655	1.3589	1.3536	1.3486	1.3377	1.3156	1.2972	1
	8.3146	8.1884	8.0843	8.0489	8.0688	8.2207	8.5608	8.7760	2
	21.623	21.3649	20.9543	20.5375	20.1238	19.3096	18.1247	17.3698	3
	21.886	21.8317	21.7425	21.7366	21.7903	22.0133	22.4835	22.8359	4
	39.732	39.1649	38.9237	38.8721	38.9840	39.6064	41.2161	42.5088	5
2.0	1.2762	1.2534	1.2493	1.2462	1.2433	1.2362	1.2192	1.2042	1
	7.6640	7.5082	7.4456	7.4410	7.4827	7.6569	7.9954	8.1987	2
	19.481	19.3740	19.0281	18.6879	18.3509	17.6805	16.6833	16.0361	3
	20.088	19.8607	19.8434	19.8803	19.9602	20.2011	20.6451	20.9602	4
	36.403	35.8065	35.6584	35.6729	35.8295	36.4892	38.0541	39.2680	5
5.0	1.1722	1.1594	1.1571	1.1556	1.1542	1.1498	1.1367	1.1242	1
	7.0111	6.9351	6.9038	6.9224	6.9799	7.1683	7.5003	7.6916	2
	17.527	17.5049	17.2438	16.9774	16.7075	16.1584	15.3217	14.7698	3
	18.391	18.2274	18.2281	18.2804	18.3695	18.6087	19.0135	19.2880	4
	33.262	32.9360	32.8594	32.9239	33.1120	33.7872	35.2781	36.3955	5
10	1.1130	1.1074	1.1061	1.1054	1.1047	1.1013	1.0897	1.0783	1
	6.6562	6.6234	6.6086	6.6401	6.7072	6.9053	7.2355	7.4201	2
	16.686	16.6779	16.4513	16.2151	15.9722	15.4712	14.6979	14.1846	3
	17.459	17.3874	17.3964	17.4554	17.5482	17.7853	18.1691	18.4234	4
	31.575	31.4357	31.3977	31.4924	31.7030	32.4012	33.8761	34.9547	5

with constants C_1, \dots, C_6 and

$$\alpha_j = (\omega^2 I_{11}^* + \eta_j B_{11}^*) / (\omega^2 I_{12}^* + \eta_j B_{12}^*);$$

$$\beta_j = \lambda_j A_{33}^* / (\omega^2 I_{11}^* + \eta_j A_{33}^*); \quad j = 1, 2, 3$$

The latter expressions show that $\alpha_4 = \alpha_1; \alpha_5 = \alpha_2; \alpha_6 = \alpha_3; \beta_4 = -\beta_1; \beta_5 = -\beta_2; \beta_6 = -\beta_3$. Therefore, general solution of (17) can be rewritten in the form

$$\{z_0(x, \omega)\} = [G_0(x, \omega)]\{C\} \tag{20}$$

where $\{C\} = (C_1, \dots, C_6)^T$ and $[G_0(x, \omega)]$ is the matrix

$$\begin{bmatrix} \alpha_1 e^{k_1 x} & \alpha_2 e^{k_2 x} & \alpha_3 e^{k_3 x} & \alpha_1 e^{-k_1 x} & \alpha_2 e^{-k_2 x} & \alpha_3 e^{-k_3 x} \\ e^{k_1 x} & e^{k_2 x} & e^{k_3 x} & e^{-k_1 x} & e^{-k_2 x} & e^{-k_3 x} \\ \beta_1 e^{k_1 x} & \beta_2 e^{k_2 x} & \beta_3 e^{k_3 x} & -\beta_1 e^{-k_1 x} & -\beta_2 e^{-k_2 x} & -\beta_3 e^{-k_3 x} \end{bmatrix} \tag{21}$$

3.2. Dynamic stiffness matrix formulation

Considering a beam element as shown in figure 2, where the following nodal displacement and force vectors are introduced

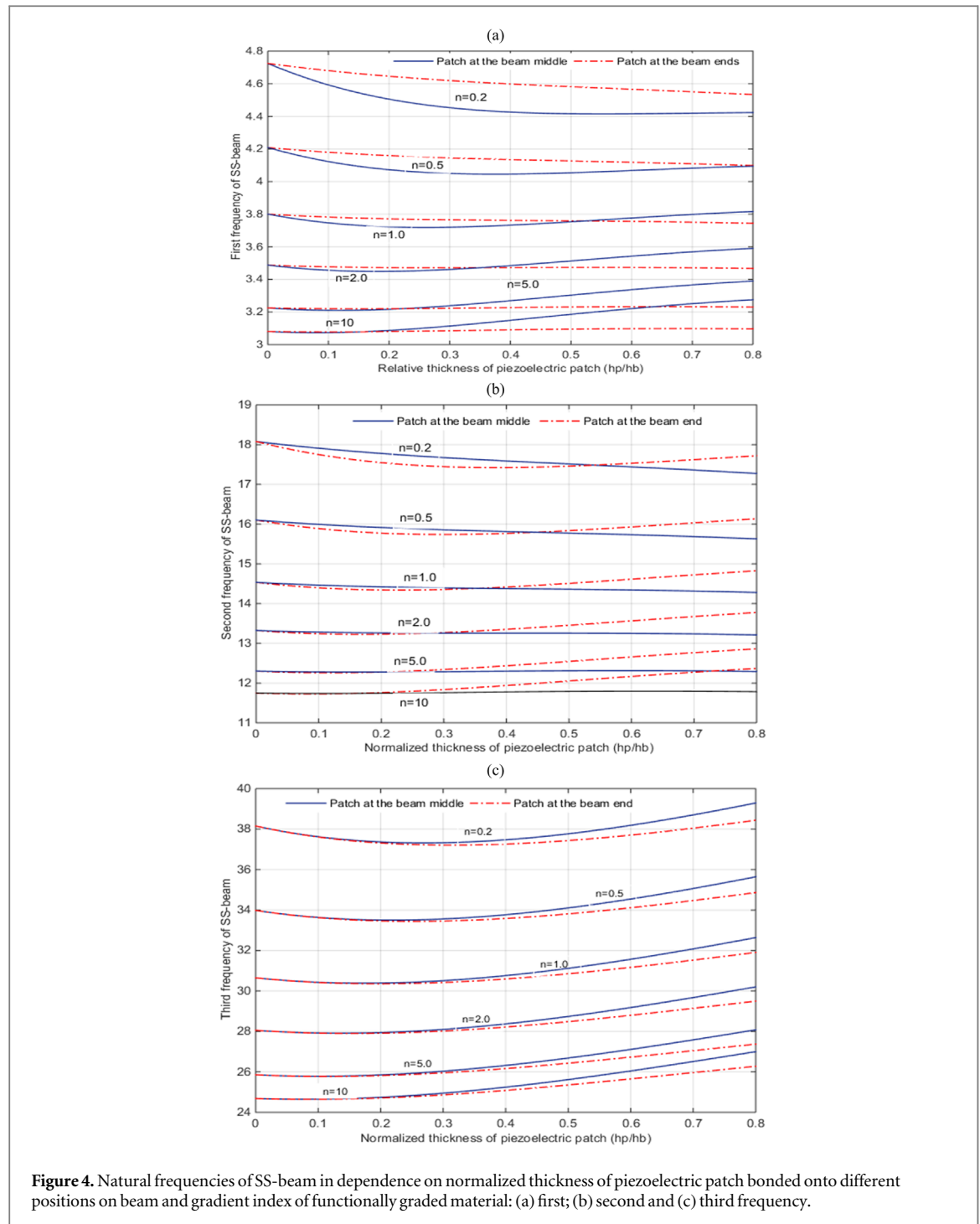


Figure 4. Natural frequencies of SS-beam in dependence on normalized thickness of piezoelectric patch bonded onto different positions on beam and gradient index of functionally graded material: (a) first; (b) second and (c) third frequency.

$$\begin{aligned} \{U_e(\omega)\} &= \{U_1, \Theta_1, W_1, U_2, \Theta_2, W_2\}^T; \\ \{P_e(\omega)\} &= \{N_1, M_1, Q_1, N_2, M_2, Q_2\}^T \end{aligned} \tag{22}$$

With

$$\begin{aligned} U_1 &= U(0, \omega); \Theta_1 = \Theta(0, \omega); W_1 = W(0, \omega); \\ U_2 &= U(L, \omega); \Theta_2 = \Theta(L, \omega); W_2 = W(L, \omega); \\ N_1 &= (B_{12}^* \partial_x \Theta - B_{11}^* \partial_x U)_{x=0}; \\ M_1 &= (B_{12}^* \partial_x U - B_{22}^* \partial_x \Theta)_{x=0}; \\ Q_1 &= A_{33}(\Theta - \partial_x W)_{x=0}; \\ N_2 &= (B_{11}^* \partial_x U - B_{12}^* \partial_x \Theta)_{x=L}; \end{aligned}$$

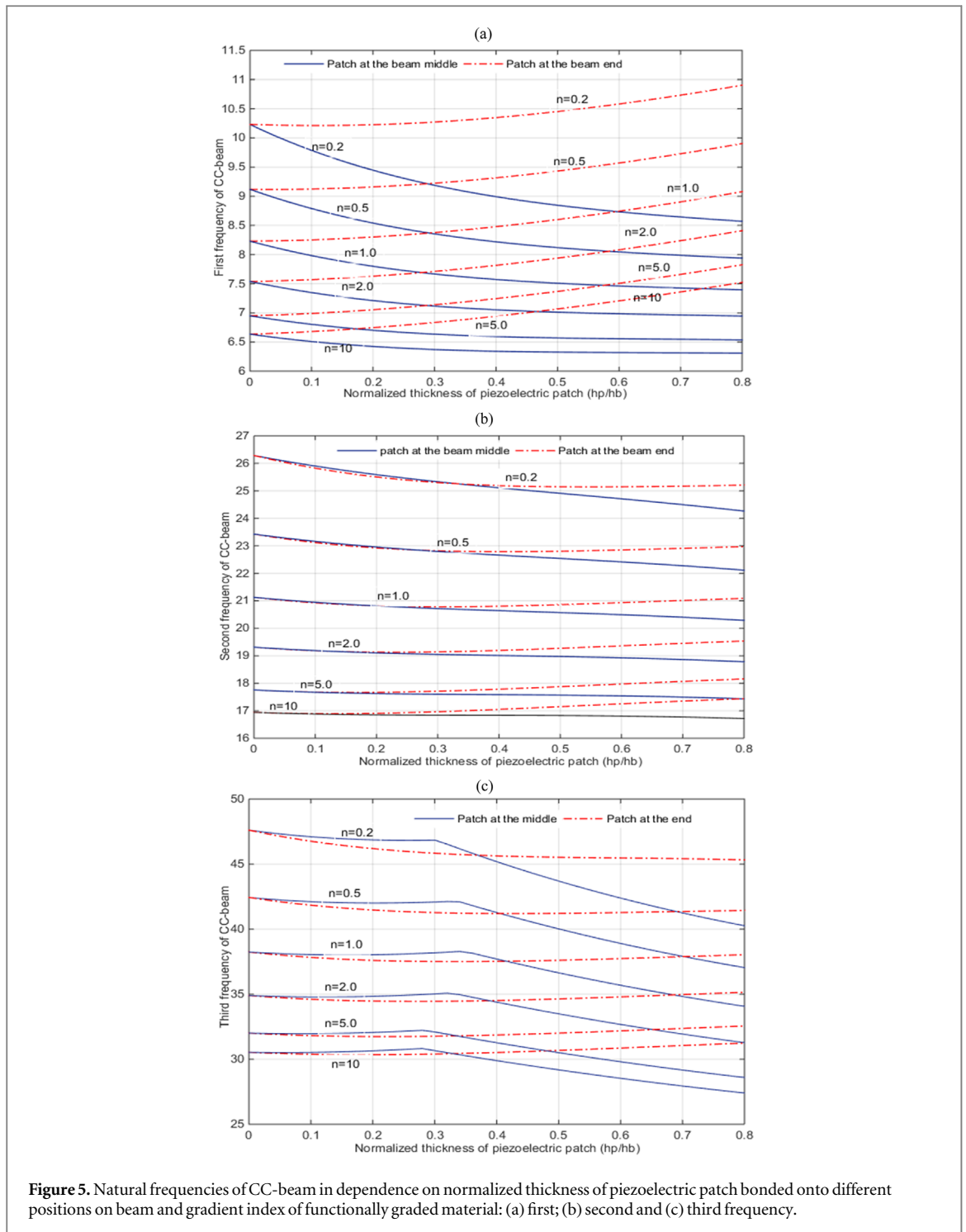


Figure 5. Natural frequencies of CC-beam in dependence on normalized thickness of piezoelectric patch bonded onto different positions on beam and gradient index of functionally graded material: (a) first; (b) second and (c) third frequency.

$$M_2 = (B_{22}^* \partial_x \Theta - B_{12}^* \partial_x U)_{x=L};$$

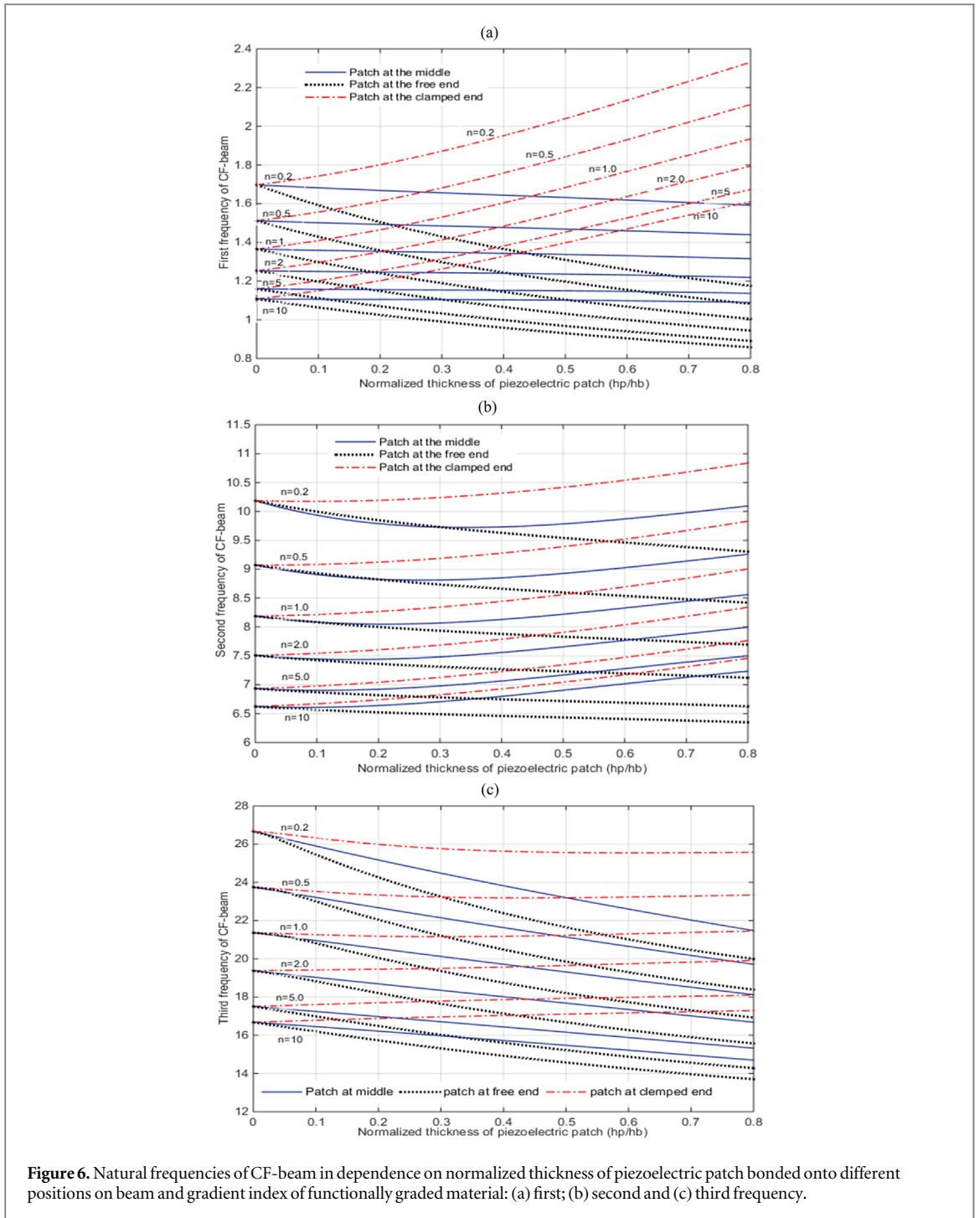
$$Q_2 = A_{33} (\partial_x W - \Theta)_{x=L}.$$

Rewrite the latter equations in matrix form

$$\{U_1, \Theta_1, W_1, U_2, \Theta_2, W_2\}^T = [Z(\omega)] \{C\}; \{N_1, M_1, Q_1, N_2, M_2, Q_2\}^T = [Q(\omega)] \{C\}, \tag{23}$$

where

$$[Z(\omega)] = \begin{bmatrix} \Phi(0, \omega) \\ \Phi(L, \omega) \end{bmatrix}; [Q(\omega)] = \begin{bmatrix} -\Re[\Phi(x, \omega)]_{x=0} \\ \Re[\Phi(x, \omega)]_{x=L} \end{bmatrix} \tag{24}$$



and \mathbb{R} is differential operator

$$[\mathbb{R}] = \begin{bmatrix} B_{11}^* \partial_x & -B_{12}^* \partial_x & 0 \\ -B_{12}^* \partial_x & B_{22}^* \partial_x & 0 \\ 0 & -A_{33}^* & A_{33}^* \partial_x \end{bmatrix}. \tag{25}$$

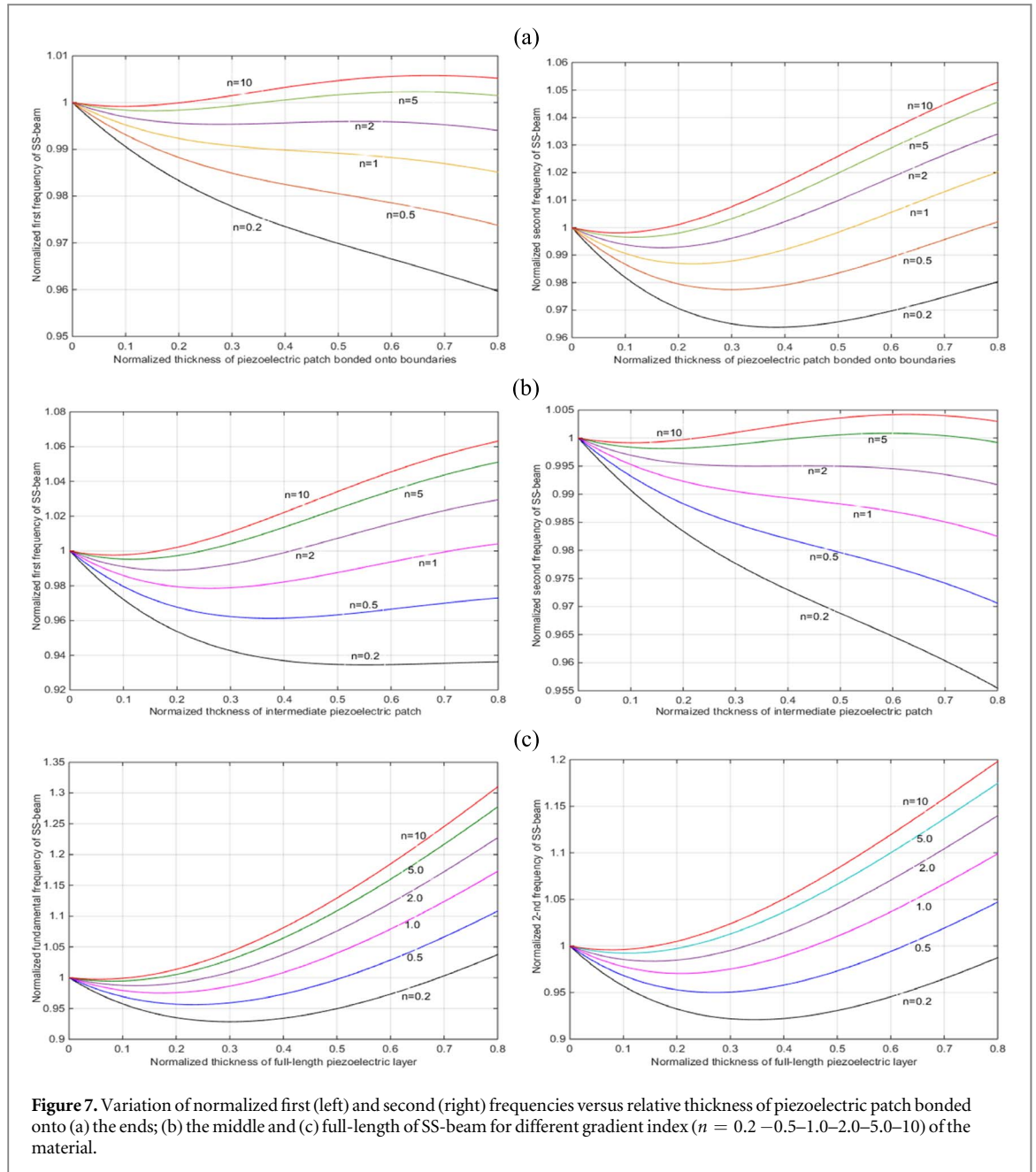
Eliminating vector C from equation (23) leads to

$$\{Q_e\} = [D_e(\omega)] \{U_e\}, \tag{26}$$

where matrix

$$[D_e(\omega)] = [Q(\omega)] \cdot [Z(\omega)]^{-1} \tag{27}$$

is called hereby dynamic stiffness matrix for the FGM Timoshenko beam element.



In general case, when a given structure consists of a number of beam elements, the total dynamic stiffness matrix for the structure is assembled accordingly to that as accomplished in the finite element method. Namely, the dynamic stiffness matrix is assembled by

$$[\mathbf{D}(\omega)] = \sum_{ne}^{e=1} [\mathbf{T}_e]^{-1} [\mathbf{D}_e(\omega)] \cdot [\mathbf{T}_e]. \quad (28)$$

4. Numerical results for illustration and validation

Consider an FGM beam bonded by a piezoelectric patch as shown in figure 3. Recalling the notations for size (thickness and length) of the piezoelectric patch and host beam, we can note that the single beam segment without piezoelectric patch is a particular case of the two-layer one when $h_p = 0$. So that the FGM beam bonded with a piezoelectric patch is now considered as a structure consisting of three beam elements, one of which is the beam element with piezoelectric layer considered above the other two elements are simple ones without piezoelectric layer. Position of piezoelectric patch bonded on beam is defined by the distance measured from the left end of beam to the left end of piezoelectric patch. The particular case considered below is that shown in

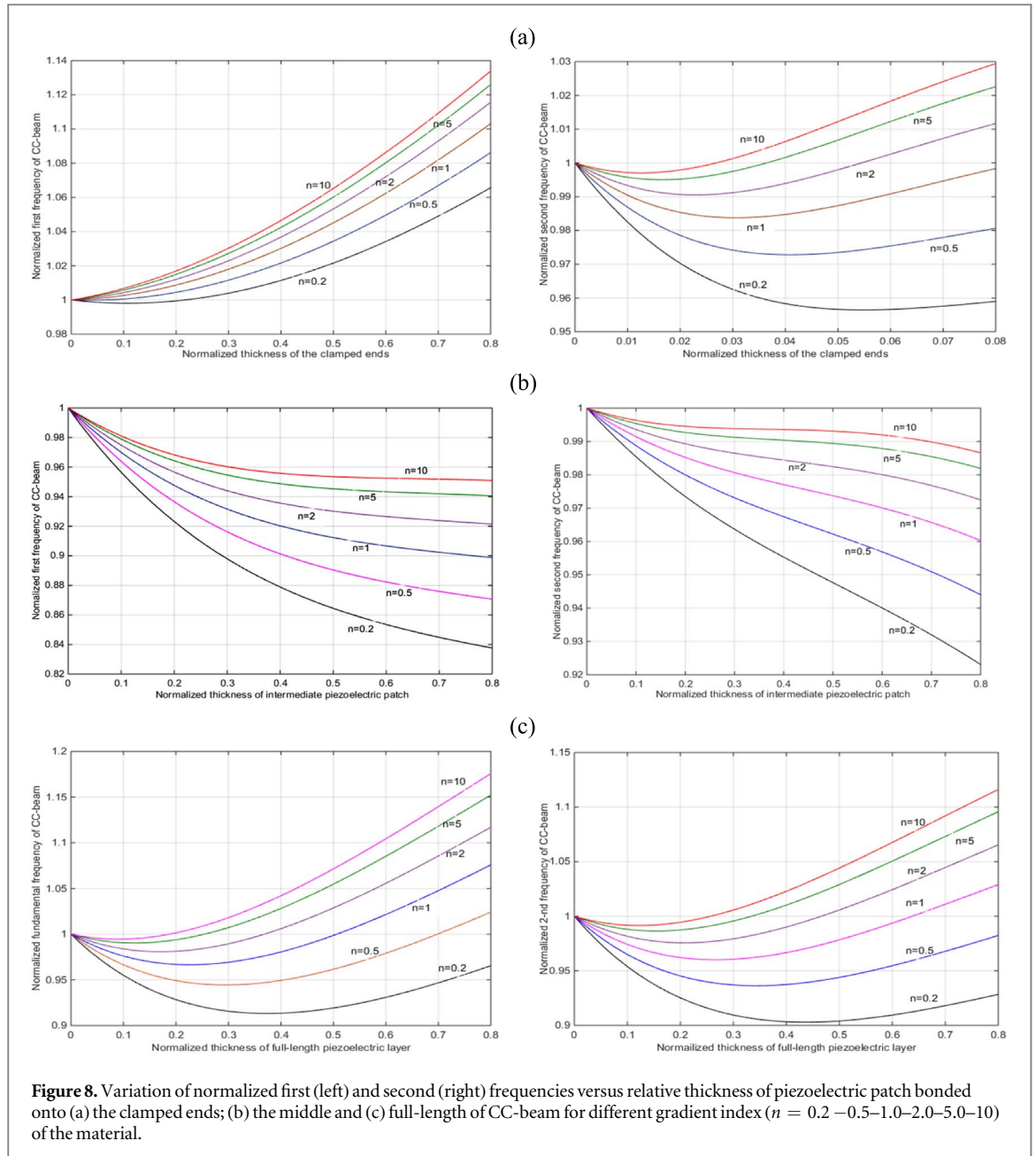


Figure 8. Variation of normalized first (left) and second (right) frequencies versus relative thickness of piezoelectric patch bonded onto (a) the clamped ends; (b) the middle and (c) full-length of CC-beam for different gradient index ($n = 0.2 - 0.5 - 1.0 - 2.0 - 5.0 - 10$) of the material.

figure 3 where length of three elements is the same and position of piezoelectric patch is acknowledged as the left, right (boundary) and intermediate (middle) one.

Suppose that constants of FGM and piezoelectric material are

$$E_t = 390 \text{ GPa}, \quad \rho_t = 3960 \text{ kg m}^{-3}, \quad \mu_t = 0.25; \quad E_b = 210 \text{ GPa},$$

$$\rho_b = 7800 \text{ kg m}^{-3}, \quad \mu_b = 0.31; \quad C_{11}^p = 69.0084 \text{ GPa},$$

$$C_{55}^p = 21.0526 \text{ GPa}, \quad \rho_p = 7750 \text{ kg m}^{-3},$$

$$h_{13} = -7.70394 \times 10^8 \text{ V m}^{-1}, \quad \beta_{33}^p = 7.3885 \times 10^7 \text{ m F}^{-1}.$$

So, natural frequency parameter $\lambda = \omega(L^2/h) \sqrt{\rho_b/E_b}$ are computed as function of thickness ratio h_p/h_b (called below normalized thickness of piezoelectric patch) for various gradient index n of the material. Five lowest frequency parameters computed for three traditional cases of boundary conditions such as simply supported (SS), clamped-clamped (CC) and clamped-free (CF) end beam are given in tables 1–3. For comparison, there are provided also in the tables the frequency parameters computed for the FGM beam without piezoelectric patch by DSM proposed in Su and Banerjee, 2015 that is shortly noticed in the Tables as S&B. Agreement between the frequency parameters computed in the present study for the case if $h_p = 0$ and those obtained in the Reference mentioned above is a fact that validates reliability of the proposed theoretical development. Also, three lowest natural frequencies of the beams in dependence of the normalized thickness of

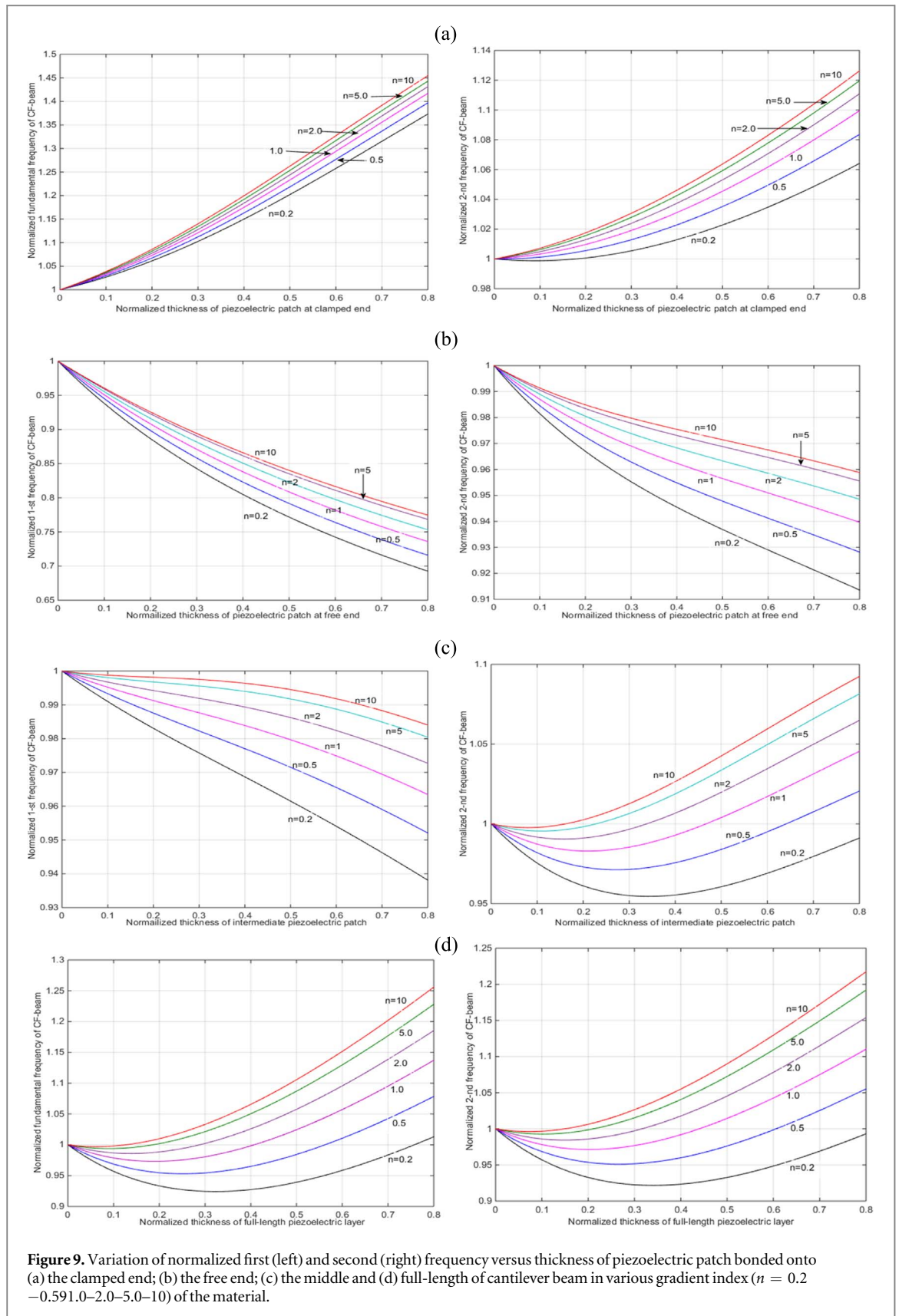


Figure 9. Variation of normalized first (left) and second (right) frequency versus thickness of piezoelectric patch bonded onto (a) the clamped end; (b) the free end; (c) the middle and (d) full-length of cantilever beam in various gradient index ($n = 0.2 - 0.591.0-2.0-5.0-10$) of the material.

the piezoelectric patch bonded on various positions on beam and gradient index of the functionally graded material are illustrated in figures 1–3.

For illustrating a more typical effect of the piezoelectric patch on variation of natural frequencies, the ratio of natural frequencies of beam with piezoelectric patch to those of beam without the patch is introduced and acknowledged herein as normalized natural frequencies. The ratio computed for two modes of FGM beam with

piezoelectric patch bonded on three different positions (two at boundaries and one at the middle) and the beam with full-length bonded piezoelectric layer is presented in the subsequent figures 4–6. The latter figures are provided in two columns representing two the frequencies and four rows corresponding to the locations where the piezoelectric patch is bonded onto. Since the boundary conditions of SS- and CC-beams are symmetrical, natural frequencies are independent upon which end the piezoelectric patch is bonded on. So that in the figures 4–5 corresponding to SS- and CC-beams there are only three rows, while in figure 6 representing the normalized frequencies of CF-beam we have got four rows.

Observing the data given in tables 1–3 and figures 4–6 one can make a discussion as follows: comparing the natural frequencies computed in this study for FGM beam with piezoelectric patch of zero thickness with those computed for FGM beam without piezoelectric patch given in Su and Banerjee, 2015 shows very good agreement between the results. This can be acknowledged as a validation of the theory developed above for FGM beam with piezoelectric patch. Natural frequencies of an FGM beam bonded with a piezoelectric patch remain to decrease with increasing gradient index n of the material as those of the beam without piezoelectric patch. Natural frequencies of FGM beam bonded with piezoelectric patch as function of the patch thickness are dependent on boundary conditions and where the piezoelectric patch is bonded on beam. Namely, for the beam of symmetric boundary conditions such as SS- and CC-beams, first two natural frequencies are both monotonically decreasing with increasing thickness of piezoelectric patch bonded onto the beam middle. In the case when the piezoelectric patch is attached to the clamped ends of CC-beam, first frequency of the beam is monotonically increasing while second and third frequencies are monotonically decreasing. In the latter case, all three natural frequencies of SS-beam are varying not monotonically, but first slightly decreasing then increasing with the thickness. More attractive behavior is observed for natural frequencies of CF-beam that are all monotonically reducing with growing of the patch thickness when the piezoelectric patch is bonded to the beam free end. While the first and second frequencies are both monotonically growing when the patch is attached to the clamped end. This was well known fact in studying cantilever beam with attached mass.

A more fruitful insight to the variation of natural frequencies versus thickness of piezoelectric patch and gradient index of material can be provided by examining the ratio of natural frequencies of beam with piezoelectric patch to those of the base beam alone. The ratios called above normalized frequencies are computed in dependence upon thickness of the piezoelectric patch for various material gradient index and different patch locations. Graphs of the normalized natural frequencies given in figures 7–9 corresponding to the cases of conventional boundary conditions allow one to make the following notices. First, it is observed that the ratios are increasing with material gradient index n what is opposite to the variation of the natural frequencies themselves. Next, the normalized natural frequencies of beam covered with full-length piezoelectric layer vary in the same (parabolic) mode for all the three cases (SS/CC/CF) of boundary conditions. A similar (to the latter) mode of variation appears also for second frequency of SS- and CC-beam with piezoelectric patch bonded onto the beam ends. The normalized first frequency of CC- and CF- beams with piezoelectric patch bonded onto clamped end is monotonically increasing with the patch thickness. Both two normalized frequencies of CC-beam with intermediately bonded piezoelectric patch and CF-beam with the patch bonded onto free end are monotonically decreasing when the thickness is growing. Finally, the normalized frequencies of SS-beam with piezoelectric patch are varying in non-monotonous mode, but it can be noticed herein that variation of the normalized first frequency along thickness of piezoelectric patch attached to the beam end is similar to variation of normalized second frequency when the patch is intermediately bonded on the beam.

All the above made notices demonstrate the fact that effect of a bonded piezoelectric patch on the dynamic characteristics of an FGM beam is strongly coupled with the effect of functionally graded material properties. This exhibits an interaction between the electro-elasticity of piezoelectric and functionally graded materials.

5. Conclusions

Natural frequencies are examined for an FGM beam bonded with a piezoelectric patch that includes also the case of beam covered with full-length piezoelectric layer using the dynamic stiffness method. First, a model of FGM beam element with a piezoelectric layer is proposed using the power law of material property grading and Timoshenko beam theory. The piezoelectric layer has the same width as the host beam and is modeled as a homogeneous Timoshenko beam element. The dynamic stiffness model of the beam element is first developed and then used for modal analysis of the FGM beam with piezoelectric patch as a multistep beam structure.

Numerical analysis has been carried out to study dependence of the natural frequencies on the piezoelectric patch thickness, location and gradient index of the functionally graded material. It was demonstrated that piezoelectric patch bonded to a beam does not change the basic properties of the beam material, but it can make change (either increase or decrease) in natural frequencies of the beam. Namely, piezoelectric patch makes the

natural frequencies increased/decreased when it is bonded closely to the clamped/free end of beam. In general, thin/thick piezoelectric patch or layer reduces/increases the stiffness of the beam.

The sensor and actuator problem of the piezoelectric patch has not been investigated in the present work; it would be a subject for further study of the authors.

Acknowledgments

This research was funded by Vietnam Academy of Science and Technology under project of number VAST01.02.18-19.

ORCID iDs

Nguyen Tien Khiem  <https://orcid.org/0000-0001-5195-2704>

References

- [1] Birman V and Byrd L M 2007 Modeling and analysis of functionally graded materials and structures *Appl. Mech. Rev.* **60** 195–216
- [2] Gupta A and Talha M 2015 Recent development in modeling and analysis of functionally graded materials and structures *Prog. Aerosp. Sci.* **79** 1–14
- [3] Chakraborty A and Gopalakrishnan S 2003 A spectrally formulated finite element for wave propagation analysis in functionally graded beams *Intern. J. of Solids and Struct.* **40** 2421–48
- [4] Li X F 2008 A unified approach for analyzing static and dynamic behaviors of functionally graded Timoshenko and Euler–Bernoulli beams *J. Sound Vib.* **318** 1210–29
- [5] Sina S A, Navazi H M and Haddadpour H 2009 An analytical method for free vibration analysis of functionally graded beams *Material & Design* **30** 741–7
- [6] Su H and Banerjee J R 2015 Development of dynamic stiffness method for free vibration of functionally graded Timoshenko beam *Computers & Structures* **147** 107–16
- [7] Sari M, Shaat M and Abdelkefi A 2017 Frequency and mode veering phenomena of axially functionally graded non-uniform beams with nonlocal residuals *Compos. Struct.* **163** 280–92
- [8] Yang J and Chen Y 2008 Free vibration and buckling analyses of functionally graded beams with edge cracks *Composite Structure* **83** 48–60
- [9] Akbas S D 2013 Free vibration characteristics of edge cracked functionally graded beams by using finite element method *International Journal of Engineering Trends and Technology* **4** 4590–7
- [10] Aydin K 2013 Free vibration of functionally graded beams with arbitrary number of surface cracks *European Journal of Mechanics A/Solid* **42** 112–24
- [11] Khiem N T, Huyen N N and Long N T 2017 Vibration of cracked Timoshenko beam made of functionally graded material *Shock & Vibration, Aircraft/Aerospace, Energy Harvesting, Acoustics & Optics Conference Proceedings of the Society for Experimental Mechanics Series 9* ed J Harvie and J Baqersad (Springer, Cham) pp 133–43
- [12] Lien T V, Duc N T and Khiem N T 2017 Free and forced vibration analysis of multiple cracked FGM multispan continuous beams using the dynamic stiffness method. *Latin American Journal of Solids and Structures* **14** 1752–66
- [13] Lien T V, Duc N T and Khiem N T 2019 Free vibration analysis of multiple cracked functionally graded Timoshenko beams *Latin American Journal of Solids and Structures* **16** e157
- [14] Yu Z G and Chu F L 2009 Identification of crack in functionally graded material beams using the p-version of finite element method *J. Sound Vib.* **325** 69–84
- [15] Banerjee A, Panigrahi B and Pohit G 2016 Crack modelling and detection in Timoshenko FGM beam under transverse vibration using frequency contour and response surface model with GA *Nondestruct. Test. Eval.* **31** 142–64
- [16] Khiem N T and Huyen N N 2017 A method for crack identification in functionally graded Timoshenko beam *Nondestruct. Test. Eval.* **32** 319–41
- [17] Tzou H S and Tseng C I 1990 Distributed piezoelectric sensor/actuator design for dynamic measurement/control of distributed parameter systems: a piezoelectric finite element approach *J. Sound Vib.* **138** 17–34
- [18] Lee C K and Moon F C 1990 Modal Sensors/Actuators *Journal of Applied Mechanics, Transactions of ASME* **57** 434–41
- [19] Rao S S and Sunar M 1994 Piezoelectricity and its use in disturbance sensing and control of flexible structures: a Survey *ASME App. Mech. Rev.* **47** 113–23
- [20] Lee J S and Jiang L Z 1996 Exact electro-elastic analysis of piezoelectric laminae via state space approach *Intern. J. of Solids and Struct.* **33** 977–90
- [21] Winston H A, Sun F and Annigeri B S 2000 *Structural Health Monitoring with Piezoelectric Active Sensors. Procc. ASME Turbo Expo 2000 4 (Munich Germany, May 8-11, 2000)* (ASME) (<https://doi.org/10.1115/2000-gt-0051>)
- [22] Bhalla S and Soh C K 2006 Progress in structural health monitoring and non-destructive evaluation using piezo-impedance transducers *Smart Material and Structures: New Research* ed P L Reece (New York: Nova Science Publishers Inc.) ch 6 177–228
- [23] Wang Q and Quek S T 2002 Enhancing flutter and buckling capacity of column by piezoelectric layers *Intern. J. of Solids and Struct.* **39** 4167–80
- [24] Wang Q, Duan W H and Quek S T 2004 Repair of notched beam under dynamic load using piezoelectric patch *Int. J. Mech. Sci.* **46** 1517–33
- [25] Mateescu D, Han Y and Misra A 2007 Dynamics of structures with piezoelectric sensors and actuators for structural health monitoring *Key Eng. Mater.* **347** 493–8
- [26] Crawley E F and De Luis J 1987 Use of piezoelectric actuators as elements of intelligent structures *AIAA J.* **25** 1373–85
- [27] Wang Q and Wang C M 2000 Optimal placement and size of piezoelectric patches on beams from the controllability perspective *Smart Mater. Struct.* **9** 558–67

- [28] Yang S M and Lee Y J 1994 Modal analysis of stepped beams with piezoelectric materials *J. Sound Vib.* **176** 289–300
- [29] Maurini C, Porfiri M and Pouget J 2006 Numerical method for modal analysis of stepped piezoelectric beams *J. Sound Vib.* **298** 918–33
- [30] Wang Q and Quek S T 2000 Flexural vibration analysis of sandwich beam coupled with piezoelectric actuator *Smart Material and Structures* **9** 103–9
- [31] Lee U and Kim J 2000 Dynamics of elastic-piezo-electric two-layer beams using spectral element method *Intern. J. of Solids and Struct.* **37** 4403–17
- [32] Park H W, Kim E J, Lim K L and Sohn H 2010 Spectral element formulation for dynamic analysis of a coupled piezo-electric wafer and bean system *Comput. Struct.* **88** 567–80
- [33] Lee U, Kim D and Park I 2013 Dynamic modeling and analysis of the PZT-bonded composite Timoshenko beams: spectral element method *J. Sound Vib.* **332** 1585–609
- [34] Khorramabadi M K and Nezamabadi A R 2010 Stability of functionally graded beams with piezoelectric layers based on the first order shear deformation theory *World Academy of Science, Engineering and Technology* **47** 527–30
- [35] Li Y S, Feng W J and Cai Z Y 2014 Bending and free vibration of functionally graded piezoelectric beam based on modified strain gradient *Compos. Struct.* **115** 41–50
- [36] Bendine K, Boukhoulda F B, Nouari M and Satla Z 2016 Active Vibration control of functionally graded beams with piezoelectric layers based on higher order shear deformation theory *Earthquake Engineering and Engineering Vibration* **15** 611–20